Water content of carbon dioxide at hydrate forming conditions

Jonathan D. Wells[a], Ahmad A.A. Majid[a,b], Jefferson L. Creek[a], E. Dendy Sloan[a], Sharon E. Borglin[c], Timothy J. Kneafsey[c], and Carolyn A. Koh[a]*

[a] Center for Hydrate Research, Chemical and Biological Engineering Department, Colorado School of Mines, Golden, Colorado 80401, USA. Email: ckoh@mines.edu

[b] Faculty of Chemical & Natural Resources Engineering, Universiti Malaysia Pahang, Malaysia

[c] Lawrence Berkeley National Laboratory, 1 Cyclotron Rd, Berkeley, CA 94720, USA

Abstract

There is an interest to ensure sub-saturated water content in lines containing carbon dioxide in applications such as enhanced oil recovery and carbon sequestration, to reduce risks of hydrate blockage and corrosion. The water content of carbon dioxide at various temperature and pressures has been measured in the past, but there is no consistent set of measurements that could be used for carbon dioxide storage and transportation design work. The solubility of water in a carbon dioxide rich gas phase at hydrate forming conditions was measured in this work. Pressures ranged from 12.06 to 29.30 bar along two isotherms, 1°C and -7°C, all within the gaseous

carbon dioxide and hydrate stability zone. For the first time in these types of measurements, the solid phase was also characterized and confirmed to be carbon dioxide hydrate via X-ray computed tomography, simultaneous with water content measurements of the gas phase. Once carbon dioxide hydrate conversion had reached a maximum value (65% estimated by X-ray computed tomography), the equilibrium water content was measured. Prior to reaching this maximum carbon dioxide hydrate conversion, the water content in carbon dioxide was observed to decrease as liquid water converted to carbon dioxide hydrate. This slow conversion to hydrate, metastability of the hydrate phase, or unexpected phases may be responsible for the large discrepancy between prior data sets for similar carbon dioxide water content measurements.

Keywords

Carbon dioxide, clathrate hydrate, water content, metastability, X-ray Computed Tomography

1. Introduction

Various applications, like enhanced oil recovery and carbon sequestration, depend on flowing nearly pure carbon dioxide through lines. With anthropogenic carbon emissions on the rise every year, there are lots of efforts being made to remove carbon dioxide from the atmosphere before irreversible damage is done.[1–4] While there are various techniques for capturing carbon dioxide from the atmosphere into a concentrated stream so

that is may be sequestered, in nearly all of them carbon dioxide must be transported from where it is captured to where it will be stored.[5–7] [8] In particular for subsea applications, carbon dioxide will have to be transported through the ocean at low temperatures and high pressures.[9,10] It is important that these lines stay clear and maintain flow, as downtime is both expensive and can pose safety concerns.[11]

Even in a nearly pure carbon dioxide stream, gas hydrate can form and accumulate with very small (ppm) amounts of water in the line.[12] Gas hydrates are ice-like crystalline compounds that form at the thermodynamic conditions found in many gas pipelines, allowing hydrates to form in and potentially block gas flow lines.[12] Hydrates are both costly to remove from a line and also pose a large safety hazard for operation, so they must be carefully managed or preferably avoided.[13,14] In gas transportation with already low water content, like carbon dioxide, it is common to dry gas below the water saturation pressure to avoid a free water phase and hydrate formation.[15,16] In order for this drying scheme to work, the water content of gas in equilibrium with hydrate must be accurately known so the gas may be dried below this value to prevent any formation.

The carbon dioxide hydrate phase boundary is well understood. Initial measurements began in the Donald L. Katz group in the 1940s[17] and have continued with others up through 2000.[18–20] Values are well established and in good agreement for the P-T location of the phase boundary. More recent carbon dioxide hydrate data has been published, but mostly in gas

mixtures as applications like hydrate based separations and carbon sequestration have received more focus.[21,22]

While P-T equilibrium measurements for hydrates are quite common, very few studies consider the water content of the bulk gas phase. In particular, for carbon dioxide, there are only a few data sets in the open literature, many of which are in disagreement with one other as seen in Figure 1.

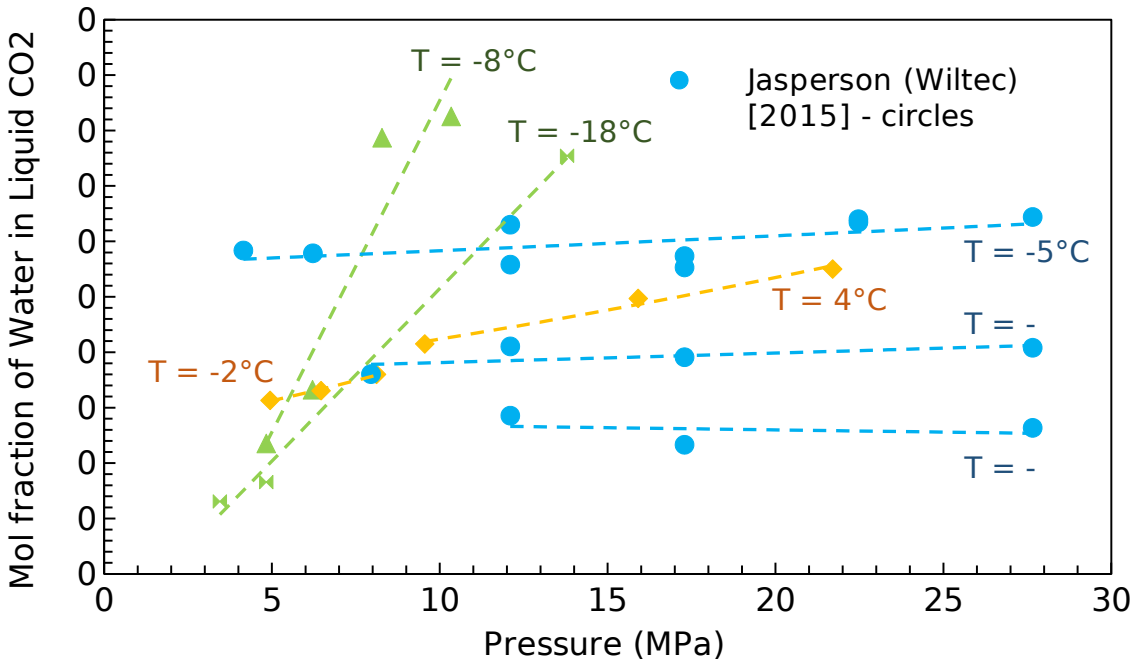

Figure 1- Literature data for saturated water content in liquid carbon dioxide as a function of pressure. Each linear fit represents an isotherm given next to line. Blue circles are from Wiltec[23], orange diamonds are from Chapoy[20], and green triangles are from Song & Kobayashi[19].

The Kobayashi group was one of the first to make these measurements in 1986, utilizing a stirred autoclave equilibrium cell.[23] The liquid CO_2 phase water content data shows a strong, unexpected, function of pressure

for water content as seen by the triangles in Figure 1. Further data showing this same trend was presented in a 2019 GPA Midstream technical report from Song et al. [24] More recently in 2011, Chapoy et al. measured the water content of carbon dioxide, and showed no dependence on pressure in a static (non-flowing) cell with impeller mixing (diamonds in Figure 1).[25] Similarly, data from Burgass et al., all collected below the ice point, show almost no function of pressure in the liquid phase CO2 water content measurements.[26] In addition, other groups have made this measurement, like the work done by Seo et al. and Youseff et al that do not show this strong pressure dependence.[27,28] Most recently, two more groups in 2015 showed this same weak function of pressure, one using a static cell at Korea University, and another in a flowing system at Wiltec (circles in Figure 1).[29] In all of these experiments measuring water content over carbon dioxide hydrate, only the gaseous or liquid carbon dioxide phase was ever evaluated. None of these studies considered evaluating the solid phase to determine whether it is hydrate, metastable hydrate, or metastable ice/liquid water.

Hydrate and ice metastability are both well documented phenomena. [30–33] In particular, for carbon dioxide hydrate, Ripmeester's group observed that ice can exist longer than 2 days at conditions where carbon dioxide hydrate is the thermodynamically stable solid phase.[34] Additionally, these different water phases (liquid, ice, or hydrate) may have different vapor pressures. For this reason, it is important to ensure that the

103 solid phase is hydrate, while measuring the saturated water content of the
104 bulk carbon dioxide gas phase.

105 There are various analytical in-situ techniques for determining ice,
106 hydrate, or liquid water existence. For example, Raman spectrometry has
107 been successfully used in the past to discriminate between different hydrate
108 structures.[35] However, Raman measures conditions at a very small
109 sample spot (few microns) and the conventional method would be
110 challenging to also measure equilibria conditions during in a macroscopic
111 system. Conversely, X-ray computed tomography (CT) can distinguish
112 differences in densities within an entire system in a very short time.[36,37]
113 Density differences are large enough to differentiate phases during carbon
114 dioxide hydrate formation in the X-ray CT scanner. While water has a
115 specific gravity of 1, that of ice is slightly lower at 0.9, and for carbon dioxide
116 hydrate it is slightly higher at 1.1.[38]

117 In this work, the water content of carbon dioxide at hydrate forming
118 condition is measured, while the water phase is simultaneously characterized
119 in situ. Previous works have shown large discrepancies between reported
120 CO_2 water content values, and no work was performed to distinguish
121 between potential metastable solid phases. Differences in the water content
122 of CO_2 literature values may be due to the presence of a metastable liquid
123 water or ice phase instead of actual carbon dioxide hydrate. In addition to
124 making water content measurements, this work investigates the
125 metastability of water at hydrate forming conditions based on X-ray CT data

collected simultaneously with water content measurements, and high pressure differential scanning calorimetry (HP-DSC) experiments to confirm and quantify the formation of hydrate.

2. Materials and Methods

In all tests, deionized water was utilized to form the carbon dioxide hydrate. Carbon dioxide was used as the hydrate guest molecule throughout this work, at a purity of 99.9995% obtained from Airgas. The column packing was made from chenille fabric (100% cotton), available off the shelf at any fabric store.

2.1 Packed Column

In this study a packed column flowing apparatus was constructed to make phase equilibrium measurements, similar to that used by Jasperson et al.[29] Water content of the effluent carbon dioxide stream was monitored via gas chromatography (GC) at Lawrence Berkeley National Laboratory (LBNL) and gas chromatography mass spectrometry (GCMS) at the Colorado School of Mines (CSM) to ensure steady state was achieved. This continuously flowing setup eliminates much of the sampling difficulty present in a static cell.

An overview of the apparatus is given in Figure 2. Pressure and temperature were both measured at the inlet to the testing section. The key section is the aluminum tubing in the center (1.27 cm ID x 45.72 cm long) filled with the chenille packing. Carbon dioxide hydrate is assumed to form

only in this section, as it is the only place where water is present. The test section is packed with chenille fabric to increase the surface area over which carbon dioxide hydrate formation occurs. Chenille was used as packing since it does not have a microporous structure that may prevent water from converting to carbon dioxide hydrate, and it is X-ray transparent, as is the aluminum used for tubing in the testing section. This trait was important to be able to use the X-ray CT to quantify the water phase.

In most phase equilibria measurements, getting representative samples at equilibrium conditions is a major challenge. For the work performed at LBNL, an isolated section of tubing at the outlet was utilized to obtain a sample of the outlet gas. After evacuating this section, it was filled with a carbon dioxide gas sample from the effluent of the column and then heated to 110°C. After heating, the sample section filled with the heated carbon dioxide was then opened to a gas bag. Because the gas bag was only partially filled, the pressure in the bag was atmospheric. From the gas bag, a syringe was used to inject an aliquot of the sample onto a Shimadzu GC-8A gas chromatograph (GC) with a Hayesep Q packed column and thermal conductivity detector (TCD) to detect the water content of the carbon dioxide gas.

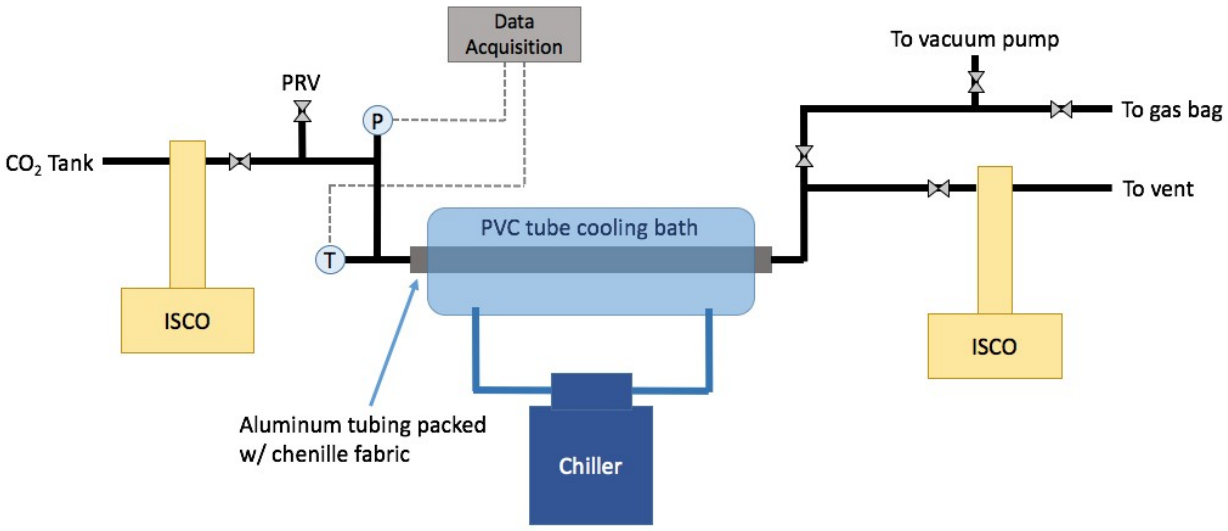

Figure 2- Schematic of the packed column apparatus developed to measure phase equilibria at hydrate forming conditions. From gas bag, sample was injected into GC for water content analysis at LBNL or directly to GCMS (no bag) at CSM.

For the experiments performed at CSM, the equilibria apparatus and GCMS are in close proximity to each other, so a small (1.5875 mm) heated line from the outlet of the aluminum testing section directly to the GCMS was utilized instead of a gas bag. This small change ensures a representative equilibrium sample is being injected into the GC column and eases the sampling procedure. Analysis at CSM was done with an Agilent 6890 Gas Chromatograph with an Agilent 5973 Mass Selective Detector and pneumatic gas injection valve. Aside from the above, the VLE saturation columns used at LBNL and CSM are identical.

To operate the packed column, the chenille fabric was first saturated with water, then loaded into the tubing. Thermal equilibrium was then reached at 1°C before the system was pressurized to 29.3 bar with carbon

dioxide to achieve hydrate forming conditions. Pressure (Transamerica 0-1500 psi transducer, 09384/CEC-1000-04) and temperature (Omega Engineering Type T thermocouple, TMQSS-062U-18) conditions were then set to the desired experimental values. To sample, the sampling section was first evacuated via a vacuum pump (Hitachi 160VP Direct Drive Rotary Vacuum) before being filled with sample and then heated to 110°C to ensure the whole sample was vaporized and to prevent condensation of water on tubing line. Finally, an aliquot of the collected sample was transferred to the GC (or GCMS at CSM) for sampling via gas bag (or directly to the heated sample line at CSM).

2.2 X-ray Computed Tomography (CT)

While measuring water content, the aluminum testing section was on the table of a GE Lightspeed 16 medical CT scanner at LBNL with X-rays of 120 kV potential. X-ray CT allows three-dimensional density distributions to be collected of the testing section while flowing CO_2 and measuring water contents at the outlet. With knowledge on the different densities between ice, liquid water, and carbon dioxide hydrate, the phases present inside the testing section can be determined.[39,40] The resolution of densities collected depends on the voxel size of 0.625 x 0.195 x 0.195 mm which results in 550 slices per scan, which in all took 2 minutes to complete.

2.3 High Pressure Differential Scanning Calorimetry (HP-DSC)

A Setaram μ-DSC VIIa micro-differential scanning calorimeter was utilized to measure water conversion to carbon dioxide hydrate. The HP-DSC has a maximum pressure of 154 bar and operating temperature of -45 to 120 ºC. In the work, measurements began by loading 1 cm x 1 cm section of chenille fabric (same as column packing) into the cell. ~15 mg of water was then added onto the fabric. To form carbon dioxide hydrate, the sample was pressurized to the test condition (29.3 bar), and then cooled to 1 °C at a rate of 0.5 °C /min. The temperature was held at 1 °C for various times (16, 24, 42 hrs) to evaluate the amount of carbon dioxide hydrate formed at different times. The temperature was increased slowly at a rate of 0.1 °C /min up to room temperature after an initial hold period to melt the carbon dioxide hydrate crystals so that the conversion could be evaluated.

3. Results and Discussion

3.1 Water Content Measurements

Carbon dioxide hydrate was first formed with the greatest driving force (highest pressure on a given isotherm), and then the pressure was isothermally lowered in order to collect water content data on water content of the CO_2 gas and hydrate formation data as a function of time and pressure. X-ray CT scans were taken approximately every 2 hours during the day and water content was measured immediately after each scan. Once the X-ray CT scans showed no further carbon dioxide hydrate formation and

the water content measurements remained constant, that water content was reported as the final equilibrium concentration.

Since the gas – hydrate region of the carbon dioxide and water phase diagram is not very large, only 2 isotherms were acquired to represent the region: one at 1°C and another at -7°C. Carbon dioxide hydrate was nucleated and annealed at 1°C before moving to the experimental temperature for both isotherms. This temperature gives the largest driving force for carbon dioxide hydrate formation, while remaining above the ice point. It was desirable to stay above the ice point as hydrate formation kinetics are much faster when forming from liquid water compared to ice. The results for both isotherms and corresponding Multiflash 6.2 Cubic Plus Association (CPA) predictions are shown in Figure 3- Equilibrium water content of gaseous carbon dioxide at hydrate conditions collected along 2 different isotherms (1 (orange) and -7°C (blue)) compared with predicted values from Multiflash CPA modelFigure 3.[41] The Multiflash CPA model combines the Soave Redlich Kwong equation of state with further terms for hydrogen bonding, making it a preferred model for gas hydrate equilibrium predictions.[42]

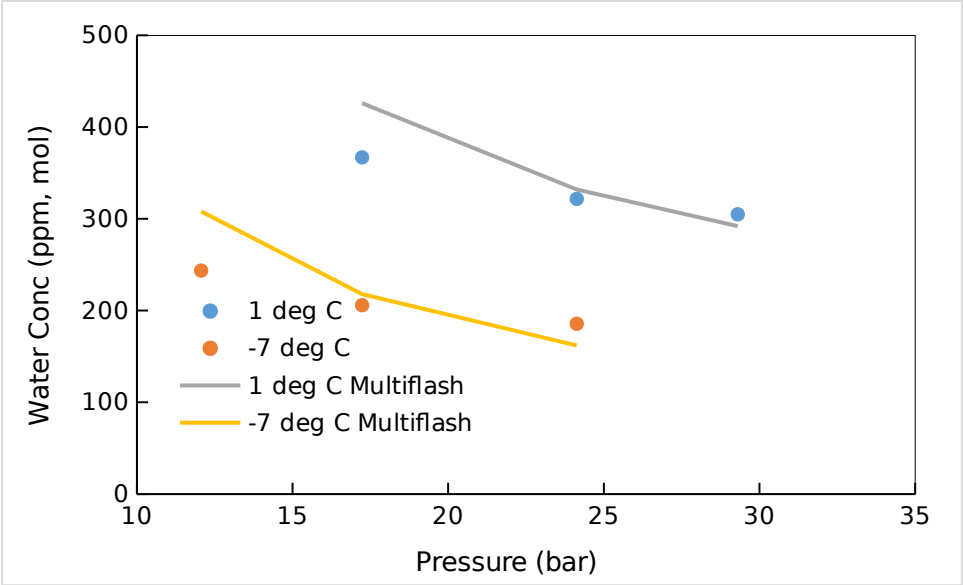

Figure 3- Equilibrium water content of gaseous carbon dioxide at hydrate conditions collected along 2 different isotherms (1 (orange) and -7°C (blue)) compared with predicted values from Multiflash CPA model with hydrate phase. Error bars represent one standard deviation from 5 replicate experiments.

Both measured isotherms show a small decrease in water concentration with pressure. The higher temperature, 1°C, shows higher water contents in the gas phase compared to the lower temperature, as expected. Vapor pressure over solids increases with increasing temperature as molecules have more kinetic energy to escape into the gas phase. Measured values are close to predicted values from Multiflash CPA and even within error (one standard deviation of 5 replicate experiments) for most points. Other phase equilibrium software designed for forecasting hydrate formation and phase properties, like in-house software CSMGEM[43] (stands for Colorado School of Mines, Gibbs Energy MinimizatioN), was evaluated and found to match Multiflash predictions almost exactly. To verify that the tube had sufficient residence time to reach equilibrium at 0.1 mL/min, the flow

rate was doubled (to 0.2 mL/min) and CO_2 water contents were measured. Water content values at the higher flowrate were within error of those measured at the original flowrate (0.1 mL/min).

Figure 4 compares the data collected in this work to previously measured values for gaseous carbon dioxide water content. Note the limited amount of data for this system; far more data is available at conditions where carbon dioxide exists as a liquid.

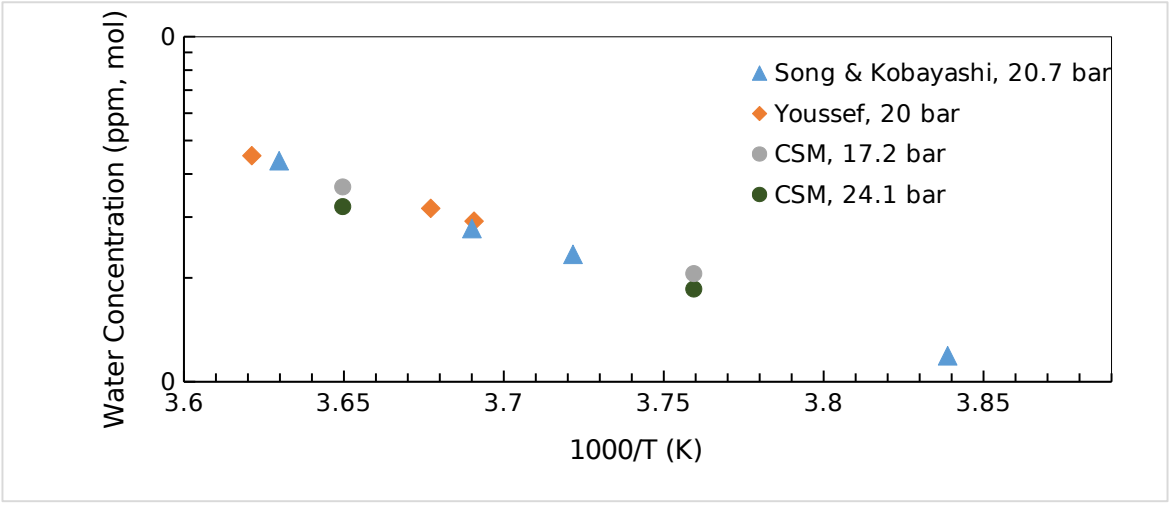

Figure 4- Comparison of measured water content (labeled CSM) in gaseous carbon dioxide (grey and green circles) to previous data collected by Youssef (orange diamonds) and Song et al (blue triangles) plotted on a log-inverse scale. Error bars on CSM data represent one standard deviation from 5 replicates and are almost smaller than the points.

The data collected in this work (error bars are one standard deviation from 5 replicates) are in agreement with water contents measured previously in other labs for similar pressures. On a plot of natural logarithm of concentration of water versus inverse absolute temperature plot, the data are all linear, as predicted by the Clausius-Clapeyron equation for a

univariant system.[44] Note that the Clausius-Clapeyron equation, normally applied to a pure component, applies equally well to this binary, but univariant system.

The data do indicate a weak function of pressure, as may be expected with a highly compressible gas phase. The highest pressure data (at CSM 24.1 bar) falls at the lowest water content compared to the other lower pressure at the corresponding temperature. While collecting the equilibrium values, X-ray CT was utilized to ensure that all liquid water had converted to carbon dioxide hydrate.

3.2 Effect of bulk water phase

While measuring the water content of carbon dioxide, CT scans were being taken at the same times. CT scanners work by measuring densities inside of each voxel in the system. Liquid water, ice, and carbon dioxide hydrate densities differ enough for them to be detected in the scanner. In this analysis, changes in density from initial conditions (liquid water and carbon dioxide gas) were evaluated. At the beginning of the experiment, a scan of the packing saturated with water was taken at ambient conditions. Then, after cooling and pressurization, further scans were taken and differences between each condition and the initial water system were taken. Colors have been assigned to the values for density differences to make viewing easier in ImageJ.[45,46] A sample of this can be seen with the CT scan in Figure 5.

Unconverted water

Tube walls

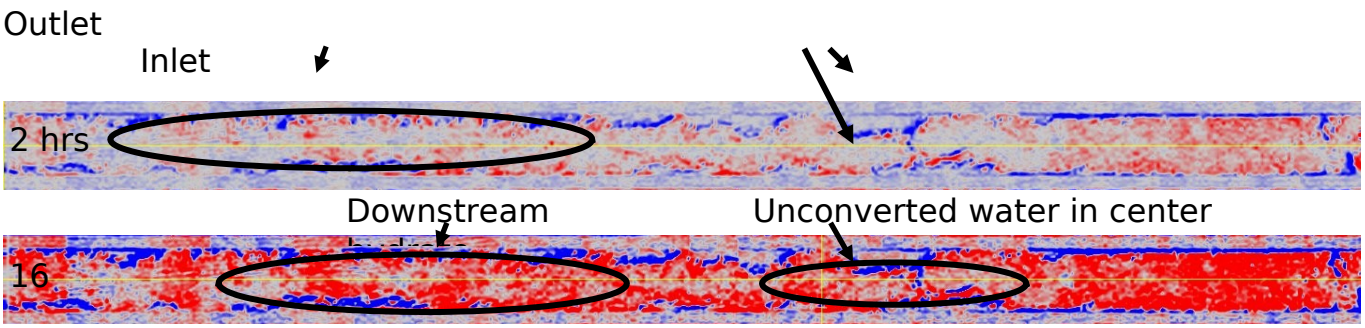

Figure 5- (top) X-ray CT scan taken 2 hours after hydrate nucleation and (bottom) X-ray CT scan taken 16 hours after hydrate nucleation at 1°C and 29.3 bar. Red represents a density increase (carbon dioxide hydrate), white is no change, and blue is a density decrease, all relative to the starting liquid water conditions (1.27 cm ID x 45.72 cm long).

This scan was taken two hours after carbon dioxide hydrate nucleation occurred and is a cross section down the center of the pipe. These scans are only differences in density between the scan taken at each time and the initial scan with liquid water. CO_2 entered the tube on the right had side, flowing to the outlet at the left at 0.1 mL/min. The tube walls can be seen at both the top and bottom of each image. Red represents an increase in density, blue represents a decrease, and white is no change. Increases in density indicate hydrate formation since carbon dioxide hydrate is denser than the original liquid water. Density decreases are due to liquid water vacating its position to move towards the carbon dioxide hydrate and being replaced by gas. Ice would be shown in Figure 5 by a lighter blue color compared to the deep blue of a liquid moving away and being replaced by a gas (larger density change). Since the differences are being taken from liquid water, white represents positions where density has not changed and liquid water still exists. It can be seen in the scan at two hours (Figure 5 top)

that there is some carbon dioxide hydrate formation on the right side, which is where carbon dioxide flowed into the system. There is still a significant amount of unconverted water (white) further downstream.

At longer times, like 16 hours after nucleation, further carbon dioxide hydrate formation has occurred. The area of red (carbon dioxide hydrate) has spread much further downstream (to the left) and less liquid water (white) remains, as seen in the bottom portion of Figure 5. There are still some white regions which contain liquid water that may be converted to carbon dioxide hydrate.

Finally, after 46 hours, the tube has become nearly all red due to carbon dioxide hydrate formation (Figure 6, top). There is almost no liquid water remaining. This can be confirmed by changing the point of reference to a later scan, at 42 hours. Because the subtraction is done at a new reference point, it is nearly all white, indicating no changes in density have occurred in those additional 4 hours. The constant density over this new time frame indicates no more carbon dioxide hydrate has formed. Both of these images can be seen in Figure 6.

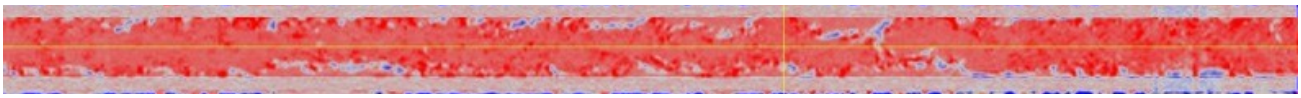

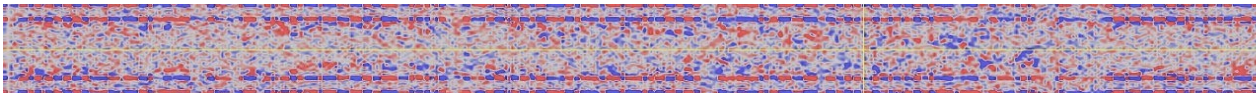

Figure 6- Top: carbon dioxide hydrate formation (in red) 46 hours after nucleation at 1°C and 29.3 bar. Bottom: Additional carbon dioxide hydrate formation from 42 to 46 hours after nucleation at 1°C and 29.3 bar. White indicates no further hydrate formation.

Further, the number of red/blue/white voxels can be quantified to be sure that nothing is changing between these two times. In Figure 7, the numbers of positive, negative, and zero valued pixels along the slice down the center of the tube were quantified for select times after nucleation with error from the standard deviation of 10 different axial slices of CT images. The plots in Figure 7 agree with what was seen in Figures 5-6, where major conversion occurs early (first 24 hrs) in the experiment, as can be seen by the sharp increase in positive density changes initially. For carbon dioxide hydrate to form, water must be consumed, as indicated by the decreasing number of zero value pixels. All of these values are constant by 42 hours after nucleation, which is consistent with the visual analysis shown in prior Figures 5-6.

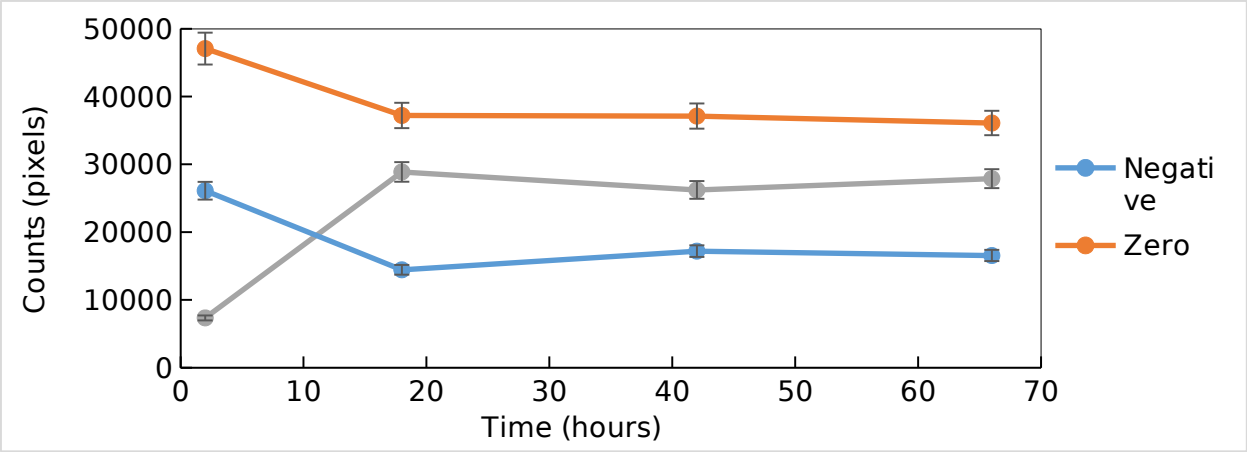

Figure 7- Changes of X-ray CT density of pixels along centerline of tube at various times after nucleation. Error bars represent one standard deviation from 10 different axial slices of the CT images.

When each X-ray CT scan was acquired, the water content in the CO_2 gas effluent was also measured. In this way, the effect of carbon dioxide hydrate versus liquid water was evaluated. The water content of carbon dioxide decreased over time as liquid water converted to carbon dioxide hydrate, as seen in Figure 8. Error bars on this plot represent one standard deviation of 5 replicate experiments. The first point is likely high due to a higher measured temperature in the cell from the exothermic hydrate reaction. This temporary increased temperature from hydrate formation would also increase the measured water content. However, the temperature returns to the setpoint value (1°C) within 2 hours and any increased water content values after that are unlikely to be due to temperature effects. While the water content slowly decreased over the first 24 hours as liquid water converted to carbon dioxide hydrate, it finally reached a constant value once carbon dioxide hydrate conversion had completed. The phase of the water

in contact with the CO_2 is very important for these measurements, as it can change the water content by nearly 50%. For this reason, the solid phase must be evaluated when making hydrate equilibrium measurements.

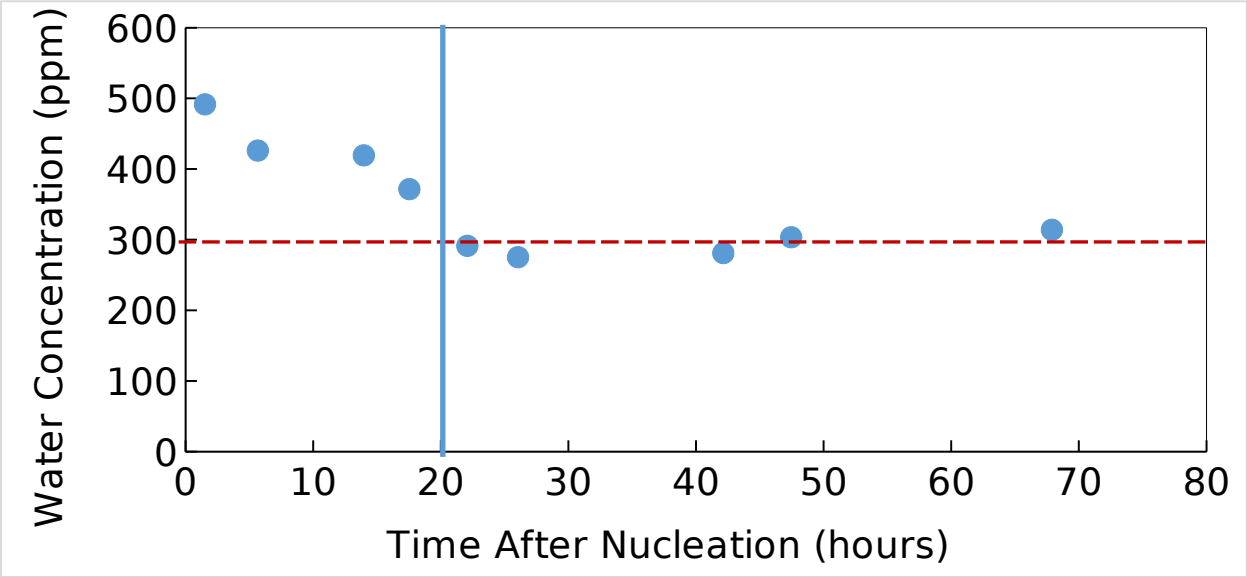

Figure 8- Water content of carbon dioxide over water (left side) and hydrate (right side) as liquid water converts to hydrate over time at 1°C and 29.3 bar. X-ray CT scans confirmed maximum carbon dioxide hydrate conversion after 40 hours. Dashed line represents Multiflash 6.2 CPA prediction (292 ppm,mol). Error bars represent one standard deviation of 5 replicate experiments.

3.3 Carbon dioxide hydrate metastability

In addition to the X-ray CT, HP-DSC was performed to confirm water metastability in the carbon dioxide hydrate forming region. Procedures for these experiments were similar to those done previously at CSM, with the exception that chenille fabric was added to the cell in order to increase surface area to improve hydrate conversion and mimic the experimental conditions in the X-ray CT. Conversion can be calculated based on the area

under the curve of the hydrate dissociation peak and knowledge of initial water amounts.[47]

Using this technique, conversion was calculated after various annealing times, which are summarized in Table 1 below. Additionally, conversion in the X-ray CT apparatus was estimated from the CT density values, like previously presented by Seol et al.[48] To calculate the conversion, the average change in density for every slice was calculated using ImageJ.[46] Next, the density change for each slice was converted to a mass with knowledge of the voxel size. The total mass increase was then summed, and with knowledge of the initial mass of water loaded into the tube and ratio of water to carbon dioxide in hydrates, the conversion can be calculated.

Table 1- Calculated carbon dioxide hydrate conversion from differential scanning calorimetry experiments and estimated conversion from X-ray CT data.

Time after Nucleation (hrs)	HP-DSC actual conversion (±5%)	X-ray CT estimated conversion (±5%)
4	No formation	23%
16	47%	39%
24	55%	64%
42	54%	65%

Similar duration experiments were necessary to achieve maximum conversion in both methods. Just like X-ray CT results, no further conversion

was seen after 24 hours in the HP-DSC. It was expected that hydrate formation in both of these apparatuses would match well, as both utilized the same packing materials and thermodynamic conditions. While the HP-DSC is a quiescent system, the flow through the tube in the X-ray CT was low enough that it was similar to the HP-DSC in terms of conversion timescales. The actual conversion is slightly higher in the X-ray CT due to the increased mass transfer from the flowing system. Due to the flowing nature of the X-ray CT experiments, the conversion can never reach 100% since some water (~300ppm level) is constantly flowing out of the system in the effluent carbon dioxide stream during experiments.

Both the X-ray CT and HP-DSC experiments eventually became mass transfer limited. There is no flow or mixing in the HP-DSC so once the water at the interface converts to carbon dioxide hydrate, the remaining liquid water inside the carbon dioxide hydrate shell will take much longer to convert to hydrate because mass transfer though the hydrate shell is slow. Similarly, the X-ray CT indicates a carbon dioxide hydrate shell forming even with a low flow rate. The carbon dioxide hydrate forms at the edge of the packing as seen in the area marked “Unconverted water in center) in Figure 5. The red (hydrate) at the edge of the fabric surrounds white (unconverted water) as a carbon dioxide hydrate shell forms around the unconverted water, slowing mass transfer and stopping any further hydrate formation. Once this shell is thick enough that it prevents any further water conversion to carbon dioxide hydrate, the gas outside the shell in the vapor phase is in

equilibrium with the carbon dioxide hydrate shell as seen by the constant water content.

4. Conclusions

When measuring water content of gases at hydrate forming conditions, it is important to not just characterize the phase in equilibrium with hydrates; the solid phase (hydrate and metastable phases) must be also considered. For the first time, water contents of gases at hydrate forming conditions were measured while simultaneously the state of the water phase present in the equilibrium. Specifically, two isotherms (1°C and -7°C) were collected between 12.06 and 29.30 bar for gaseous carbon dioxide water content in equilibrium with carbon dioxide hydrate. In order to verify values were collected in equilibrium with carbon dioxide hydrate, X-ray CT was used to simultaneously evaluate the state of the water phase. Initially, when liquid water still persisted in the system and carbon dioxide hydrate conversion was low, measured water content values were up to 50% higher than final equilibrium values. As time moved forward and further liquid water was converted to carbon dioxide hydrate, the water content of the CO_2 decreased asymptotically until reaching equilibrium values as the gas came into equilibrium with only a hydrate shell.

Water metastability within the carbon dioxide hydrate forming region was also evaluated. X-ray CT indicated that carbon dioxide hydrate took over 42 hours to achieve maximum conversion from liquid water at 29.3 bar

and 1°C. HP-DSC confirmed metastability results in the X-ray CT, as conversion in two independent apparatuses took place over similar timescales (>24 hours). Carbon dioxide hydrate conversion took so long (>24 hours) in both systems due to the large amounts of water and mass transfer limitations after maximum conversion. Water metastability is an important parameter that must be considered when making hydrate phase equilibrium measurements, as different water phases may lead to significantly different measured water content in the equilibrated fluid phase.

5. Conflicts of Interest

There are no conflicts of interest to declare.

6. Acknowledgements

The authors would like to acknowledge the GPA Midstream Associtaion for funding this work, especially Dr. Håvard Lidal from Equinor and the GPA Midstream Research Committee for their guidance. Additionally, Mike Stadick and Mike Klasner were essential for getting the systems at CSM working properly.

References

[1] L. Hughes, Biological consequences of global warming: is the signal already apparent?, Trends Ecol. Evol. 15 (2000) 56–61.

[2] T.A. Boden, G. Marland, R.J. Andres, Global, Regional, and National Fossil-Fuel CO2 Emissions, Oak Ridge, Tenn., USA, 2017.

[3] R.S. Haszeldine, Carbon Capture and Storage: How Green Can Black Be?, Science (80-.). 325 (2009) 1647–1653.

[4] K.S. Lackner, S. Brennan, J.M. Matter, A.H.A. Park, A. Wright, B. Van Der Zwaan, The urgency of the development of CO2 capture from ambient air, PNAS. 109 (2012) 13156–13162. https://doi.org/10.1073/pnas.1108765109.

[5] J. Gibbins, H. Chalmers, Carbon capture and storage, Energy Policy. 36 (2008) 4317–4322. https://doi.org/10.1016/j.enpol.2008.09.058.

[6] D. Figueroa, T. Fout, S. Plasynski, H. Mcilvried, R.D. Srivastava, Advances in CO2 capture technology — The U. S. Department of Energy’s Carbon Sequestration Program, Int. J. Greenh. Gas Control. (2008) 9–20. https://doi.org/10.1016/S1750-5836(07)00094-1.

[7] M.E. Boot-Hanford, J.C. Abanades, E.J. Anthony, M.J. Blunt, S. Brandani, Carbon Capture and Storage Update, Energy Environ. Sci. 7 (2014) 130–189. https://doi.org/10.1039/c3ee42350f.

[8] R. Svensson, M. Odenberger, F. Johnsson, L. Stromberg, Transportation systems for CO2 –– application to carbon capture and storage, Energy Convers. Manag. 45 (2004) 2343–2353. https://doi.org/10.1016/j.enconman.2003.11.022.

[9] M.D. Aminu, S.A. Nabavi, C.A. Rochelle, V. Manovic, A review of developments in carbon dioxide storage, Appl. Energy. 208 (2017)

494 1389–1419. https://doi.org/10.1016/j.apenergy.2017.09.015.

495 [10] M. Peter, N.P. Fofonoff, Conversion of pressure to depth in the ocean,
496 Deep Sea Res. 23 (1976) 109–111.

497 [11] E.D. Sloan, C. Koh, A.K. Sum, Natural Gas Hydrates in Flow Assurance,
498 First, Elsevier, 2011.

499 [12] E.D. Sloan, C.A. Koh, Clathrate Hydrates of Natural Gases, 3rd ed., CRC
500 Press, 2008.

501 [13] M.N. Lingelem, A.I. Majeed, E. Stange, Industrial Experience in
502 Evaluation of Hydrate Formation, Inhibition, and Dissociation in Pipeline
503 Design and Operation, Ann. N. Y. Acad. Sci. 715 (1994) 75–93.

504 [14] J.J. Xiao, G. Shoup, G. Hatton, V. Kruka, OTC 8728 Predicting Hydrate
505 Plug Movement During Subsea Flowline Depressurization Operations,
506 Offshore Technol. Conf. (1998) 161–170.

507 [15] A. Witkowski, A. Rusin, M. Majkut, S. Rulik, K. Stolecka, Comprehensive
508 analysis of pipeline transportation systems for CO 2 sequestration .
509 Thermodynamics and safety problems, Energy Convers. Manag. 76
510 (2013) 665–673. https://doi.org/10.1016/j.enconman.2013.07.087.

511 [16] M. Naseer, W. Brandstatter, Hydrate formation in natural gas pipelines,
512 Comput. Methods Multiph. Flow VI. 70 (2011) 261–270.
513 https://doi.org/10.2495/MPF110221.

514 [17] H.G. Donnelly, D.L. Katz, Phase Equilibria in the Dioxide-Methane

System, Ind. Eng. Chem. Res. 46 (1954) 511–517. https://doi.org/10.1021/ie50531a036.

[18] S.D. Larson, Phase studies of the two component carbon dioxide-water system involving the carbon dioxide hydrate, U. of Illinois, 1955.

[19] M. Wendland, H. Hasse, G. Maurer, Experimental Pressure - Temperature Data on Three- and Four-Phase Equilibria of Fluid , Hydrate , and Ice Phases in the System Carbon Dioxide - Water, J. Chem. Eng. Data. 44 (1999) 901–906. https://doi.org/10.1021/je980208o.

[20] S.O. Yang, I.M. Yang, Y.S. Kim, C.S. Lee, Measurement and prediction of phase equilibria for water+CO2 in hydrate forming conditions, Fluid Phase Equilib. 175 (2000) 75–89. https://doi.org/10.1016/S0378-3812(00)00467-2.

[21] S. Adisasmito, R.J. Frank, E.D. Sloan, Hydrates of Carbon Dioxide and Methane Mixtures, J. Chem. Eng. Data. 36 (1991) 68–71. https://doi.org/10.1021/je00001a020.

[22] P. Babu, P. Linga, R. Kumar, P. Englezos, A review of the hydrate based gas separation (HBGS) process forcarbon dioxide pre-combustion capture, Energy. 85 (2015) 261–279. https://doi.org/10.1016/j.energy.2015.03.103.

[23] K.Y. Song, R. Kobayashi, The Water Content of CO2-rich Fluids in

Equilibirum with Liquid Water and/or Hydrates, 1986.

[24] K.Y. Song, K.R. Cox, W.G. Chapman, Water Content in Gaseous and Liquid Carbon Dioxide and its Mixtures with Methane in Equilibrium with Hydrate, GPA Midstream Tech. Publ. (2019).

[25] A. Chapoy, R. Burgass, B. Tohidi, J.M. Austell, C. Eickhoff, Effect of Common Impurities on the Phase Behavior of Carbon-Dioxide-Rich Systems : Minimizing the Risk of Hydrate Formation and Two-Phase Flow, SPE J. 16 (2011) 921–930.

[26] R. Burgass, A. Chapoy, P. Duchet-Suchaux, B. Tohidi, Experimental water content measurements of carbon dioxide in equilibrium with hydrates at (223.15 to 263.15) K and (1.0 to 10.0) MPa, J. Chem. Thermodyn. 69 (2014) 1–5. https://doi.org/10.1016/j.jct.2013.09.033.

[27] M. Do Seo, J.W. Kang, C.S. Lee, Water Solubility Measurements of the CO2 -Rich Liquid Phase in Equilibrium with Gas Hydrates Using an Indirect Method, J. Chem. Eng. Data. 56 (2011) 2626–2629. https://doi.org/10.1021/je2001232.

[28] Z. Youssef, A. Barreau, P. Mougin, J. Jose, I. Mokbel, C.B.L. I, Measurements of Hydrate Dissociation Temperature of Methane , Ethane , and CO 2 in the Absence of Any Aqueous Phase and Prediction with the Cubic Plus Association Equation of State, Ind. Eng. Chem. Res. 48 (2009) 4045–4050.

[29] L. V Jasperson, J.W. Kang, C.S. Lee, D. Macklin, P.M. Mathias, R.J. McDougal, W.G. Rho, D. VonNiederhausern, Experimental Determination of the Equilibrium Water Content of CO2 at High Pressure and Low Temperature, J. Chem. Eng. Data. 60 (2015) 2674–2683. https://doi.org/10.1021/acs.jced.5b00320.

[30] E.D. Sloan, F. Fleyfel, Molecular Mechanism for Gas Hydrate Nucleation from Ice, AIChE J. 37 (1991).

[31] V. Natarajan, P.R. Bishnoi, N. Kalogerakis, Induction Phenomena In Gas Hydrate Nucleation, Chem. Eng. Sci. 49 (1994) 2075–2087.

[32] L.A. Stern, S. Circone, S.H. Kirby, W.B. Durham, Anomalous Preservation of Pure Methane Hydrate at 1 atm, J. Phys. Chem. B. 105 (2001) 1756–1762. https://doi.org/10.1021/jp003061s.

[33] V.P. Melnikov, A.N. Nesterov, A.M. Reshetnikov, V.A. Istomin, V.G. Kwon, Stability and growth of gas hydrates below the ice – hydrate – gas equilibrium line on the P – T phase diagram, Chem. Eng. Sci. 65 (2010) 906–914. https://doi.org/10.1016/j.ces.2009.09.041.

[34] I.L. Moudrakovski, G.E. McLaurin, C.I. Ratcliffe, J.A. Ripmeester, Methane and Carbon Dioxide Hydrate Formation in Water Droplets: Spatially Resolved Measurements from Magnetic Resonance Microimaging, J. Phys. Chem. B. 108 (2004) 17591–17595. https://doi.org/10.1021/jp0473220.

[35] H. Ohno, T.A. Strobel, S.F. Dec, E.D. Sloan, C.A. Koh, Raman Studies of Methane - Ethane Hydrate Metastability, J. Phys. Chem. A. 113 (2009) 1711–1716.

[36] J. Wang, J. Zhao, M. Yang, Y. Li, W. Liu, Y. Song, Permeability of laboratory-formed porous media containing methane hydrate : Observations using X-ray computed tomography and simulations with pore network models, Fuel. 145 (2015) 170–179. https://doi.org/10.1016/j.fuel.2014.12.079.

[37] T.J. Kneafsey, Y. Seol, A. Gupta, L. Tomutsa, Permeability of Laboratory-Formed Methane-Hydrate-Bearing Sand : Measurements and Observations Using X-Ray Computed Tomography, SPE J. (2011) 78–94.

[38] A.T. Bozzo, H.-S. Chen, J.R. Kass, A.J. Barduhn, The Properties of the Hydrates of Chlorine and Carbon Dioxide, Deslaination. 16 (1975) 303–320.

[39] V. Cnudde, M.N. Boone, High-resolution X-ray computed tomography in geosciences : A review of the current technology and applications, Earth Sci. Rev. 123 (2013) 1–17. https://doi.org/10.1016/j.earscirev.2013.04.003.

[40] T.J. Kneafsey, G.J. Moridis, X-Ray computed tomography examination and comparison of gas hydrate dissociation in NGHP-01 expedition (India) and Mount Elbert (Alaska) sediment cores : Experimental observations and numerical modeling, Mar. Pet. Geol. 58 (2014) 526–

539. https://doi.org/10.1016/j.marpetgeo.2014.06.016.

[41] KBC, Multiflash- PVT Modelling and Flow Assurance Software.

[42] G. M. Kontogeorgis, M. L. Michelsen, G. K. Folas, S. Derawi, N. von Solms, E. H. Stenby, Ten Years with the CPA (Cubic-Plus-Association) Equation of State. Part 1. Pure Compounds and Self-Associating Systems, Ind. Eng. Chem. Res. 45 (2006) 4855–4868. https://doi.org/10.1021/ie051305v.

[43] CHR, CSMGem.

[44] T.Y. Makogon, E.D. Sloan, Phase Equilibrium for Methane Hydrate from 190 to 262 K, J. Chem. Eng. Data. 39 (1994) 351–353. https://doi.org/10.1021/je00014a035.

[45] P. Thevenaz, U.E. Ruttimann, M. Unser, A Pyramid Approach to Subpixel Registration Based on Intensity, IEEE Trans. Image Process. 7 (1998) 27–41.

[46] C.A. Schneider, W.S. Rasband, K.W. Eliceiri, NIH Image to ImageJ : 25 years of Image Analysis, Nat. Methods. 9 (2012) 671–675.

[47] J.W. Lachance, Investigation of Gas Hydrates Using Differential Scanning Calorimetry with Water-In-Oil Emulsion, Colorado School of Mines, 2008.

[48] Y. Seol, T.J. Kneafsey, Methane hydrate induced permeability modification for multiphase flow in unsaturated porous media, 116

621 (2011) 1–15. https://doi.org/10.1029/2010JB008040.

622